This is an open access article published under an ACS AuthorChoice License, which permits copying and redistribution of the article or any adaptations for non-commercial purposes.

analytical chemistry

Article

Cite This: Anal. Chem. 2019, 91, 14951−14959

pubs.acs.org/ac

Polyaniline Films as Electrochemical-Proton Pump for Acidification of Thin Layer Samples

Alexander Wiorek,[†] Maria Cuartero,[†] Roland De Marco,[‡,§,∥] and Gaston A. Crespo*[,†]

[†]Department of Chemistry, KTH Royal Institute of Technology, 10044 Stockholm, Sweden

[‡]Faculty of Science, Health, Education and Engineering, University of the Sunshine Coast, 90 Sippy Downs Drive, Sippy Downs, Queensland 4556, Australia

[§]School of Chemistry and Molecular Biosciences, The University of Queensland, Brisbane, Queensland 4072, Australia

[∥]Fuels and Energy Technology Institute, Curtin University, Perth, Western Australia 6102, Australia

Supporting Information

ABSTRACT: Here, we provide the first experimental evidence of proton release from polyaniline (PANI) films subjected to anodic potentials at environmental pHs. We conducted an extensive characterization of unpolarized/polarized PANI films—synthesized by traditional sequential voltammetric scanning—by using spectroelectrochemistry, synchrotron radiation-X-ray photoelectron spectroscopy, near edge X-ray absorption fine structure, and potentiometric pH sensing in the vicinity of the PANI layer. This new insight enables the utilization of PANI as a proton pump, which is actively tuned through an electrochemical pulse, so as to controllably acidify well-confined thin layer samples. Furthermore, we demonstrate the analytical significance of this system by measuring the alkalinity of artificial and natural water samples by using two faced planar PANI electrodes, one working as a proton source and the other one as pH electrode. Finally, the impact of this approach is 2-fold: (i) all-solid-state electrode materials may be used with devisible consequences in miniaturized and implementable submersible probes, and (ii) rapid determination of alkalinity as compared to traditional approaches together with a versatility in pH adjustment in any kind of sample, among other applications.

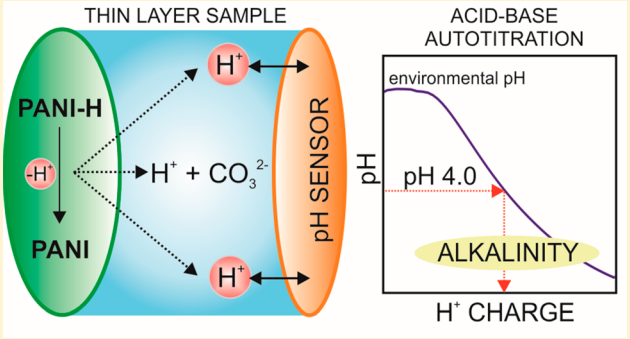

INTRODUCTION

Polyaniline (PANI) is univocally one of the most relevant electronic/conducting polymers. The possibility of tuning its physicochemical properties by diverse external stimulus (i.e., light, current, chemical doping) makes it very attractive for many applications, which rank from rechargeable batteries to biomedical sensors.[1−4] PANI's great versatility is mostly due to its remarkable flexibility in the modulation of key properties. These include conductivity, oxidation/reduction, electrochromism and porosity, oxidation state, thickness and morphology—as the rest of electrically conducting polymers—but also the degree of protonation of the PANI film.[5−7] Indeed, PANI is to be very pH sensitive, and it converts to its nonconductive form at pH ca. 3,[8,9] which is a drawback for its use as a regular electrode in low pH media but an advantage as a pH sensor.[10]

It is well-accepted today that there are three chemical structures of PANI with different oxidation states named as leucoemeraldine (LE, fully reduced), emeraldine (E, partially oxidized), and pernigraniline (PN, fully oxidized), and every oxidation state has a pair of base (-B) and salt (-S) forms according to the acid−based chemistry of PANI (see Supporting Information (SI) Figure S1). Electrochemical techniques such as cyclic voltammetry (CV) have been used to adjust the redox potential, therefore controlling the PANI state and achieving different types of films accordingly (i.e., level of conductivity and even nonconducting PANI films at convenience).[11] Furthermore, voltammetric experiments have contributed to a deep understanding of the complex mechanism of PANI's formation.[12,13]

Early experiments by MacDiarmid et al. showed CV of PANI with two reversible redox waves in HCl solution:[1,11] the first peak was attributed to oxidation of LE to E and the second one from E to PN structures, which was accompanied by loss of protons. This latter process was subsequently confirmed by other complementary techniques such as X-ray photoelectron spectroscopy (XPS),[14] probe beam deflection techniques,[15,16] electrochemical quartz crystal microbalance,[17] infrared spectroscopy,[18,19] field-effect transistor-based ion-selective sensor,[20] online mass spectrometry,[21] potentiometry,[22] and UV−vis spectroscopy.[23] Then, the implication of protons

Received: July 26, 2019
Accepted: November 6, 2019
Published: November 6, 2019

Downloaded via KTH ROYAL INST OF TECHNOLOGY on January 29, 2024 at 16:01:47 (UTC).
See https://pubs.acs.org/sharingguidelines for options on how to legitimately share published articles.

© 2019 American Chemical Society

DOI: 10.1021/acs.analchem.9b03402
Anal. Chem. 2019, 91, 14951−14959

was also linked to these LE-E-PN redox transitions through the involvement of the different acid/base forms depending on the pH of the PANI film/medium (see SI Figure S1).[8,9] It is surprising that, as far as we know, this phenomenon has not yet been applied as a possible proton reservoir in analytical applications.

Very recently, there have been reports on electrochemically controlled acid−base titrations where the sample is confined in a thin layer gap.[24,25] The electrochemical configuration consisted of two perm-selective membranes placed opposite, each to define the sample confinement: one membrane was used as the electrochemically controlled hydrogen ion pump and the other one as the potentiometric readout. A linear relationship between the duration of the applied pulse and the released charge enabled a titration of the sample mimicking a volumetric process. Significantly, this concept was applied for total alkalinity detection in river samples.[24,25] Notably, the term alkalinity refers to all titratable components down to pH 4.0 and provides valuable information on the amount of carbonate, bicarbonate, and hydroxide ions in the sample.

The knowledge of alkalinity trends plays an important role from the environmental point of view in understanding the nonnatural proliferation of microorganisms, acidification of water bodies, and the quality of water for human consumption.[26] Traditionally, these measurements have been performed ex situ in a centralized laboratory, or in the best cases, close-to-shore, using classical automated methods such as colorimetric and potentiometric acid−base titration after sampling.[24,25] However, this approach is fraught with uncertainties since it is likely that there are alterations in the samples as a result of variations in the carbon dioxide partial pressure during transportation to the laboratory, handling, and analysis.[27] Here, an in situ tool for alkalinity assessment would be beneficial.

Building on previous works,[24,25] a solid-contact material like PANI with better mechanical and chemical robustness compared to perm-selective membranes implemented in inner filling type ion-selective electrodes, is herein proposed as a superior technology for controlled proton release. Thus, we provide the first experimental evidence for proton release from PANI films subjected to anodic potentials at environmental pHs, that is, not the highly acidified conditions of previous above-mentioned studies.[14−23] Using extensive characterization of the polarization of the PANI film—synthesized with traditional sequential voltammetric scanning—by spectroelectrochemistry, synchrotron radiation-X-ray photoelectron spectroscopy (SR-XPS), near edge X-ray absorption fine structure (NEXAFS), and in situ potentiometric pH determinations in the very vicinity of the PANI layer upon polarization, we illustrate that PANI may be used as an all-solid-state proton source for rapid sample acidification and alkalinity detection. This latter is achieved using a new in situ autotitration method, as opposed to conventional ex situ and centralized laboratory titrimetric techniques.

EXPERIMENTAL SECTION

The setup to accomplish spectroelectrochemistry is depicted in Scheme 1a. The PANI-based ITO glass electrode (working electrode, WE) is placed at the bottom of the Teflon compartment, in which the solution under study is added, with the counter (CE) and reference electrode (RE) placed inside the solution. The light source and detector are aligned to the center of the WE. Scheme 1b illustrates the thin layer microfluidic cell for sample acidification, which was fabricated to locate two screen-printed electrodes (labeled as 2 and 4 and shown in Scheme 1b) in a confronted way using the 3-D printer Ultimaker 3 and the PLA substrate. One of the screen-printed electrodes is the PANI-based pH sensor[10] (see SI Figure S2 for the regular calibration graph) and the other one comprised a PANI film as a source of protons (labeled as 2 and 4). The electrodes are placed between the two marked holders (labeled as 1 and 5) and, in the gap, there is a spacer made by PLA filament (diameter of 8 mm and 200−400 μm thickness depending on the thickness of the PANI film) to confine the sample in a gap of close to ca. 100 μm in thickness (labeled as 3). The cell additionally contains one inlet and outlet thus allowing for the sample flow in the thin layer gap. The cell and spacer had a diameter of 24 mm, with an effective internal volume of ca. 35 μL. For a detailed description of the electrode fabrication, the reader is referred to the SI.

Scheme 1. (a) Illustration of the Cell for PANI Electropolymerization and Spectroelectrochemical Measurements, (b) Thin Layer Cell for Sample Acidification[a]

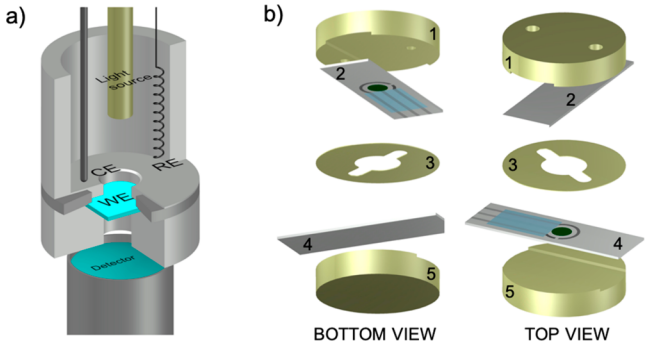

[a]WE: Working electrode (transparent ITO glass), RE: reference electrode (Ag/AgCl wire), CE: counter electrode (Pt rod), 1: electrode holder with flow inlet and outlet, 2: PANI-based electrode as proton source, 3: channel for the thin layer sample, 4: PANI-based electrode as pH senor, 5: electrode holder.

RESULTS AND DISCUSSION

Characterization of the Formation of the PANI Film on ITO Glass by Spectroelectrochemistry. Figure 1a shows the voltammograms recorded during the electro-

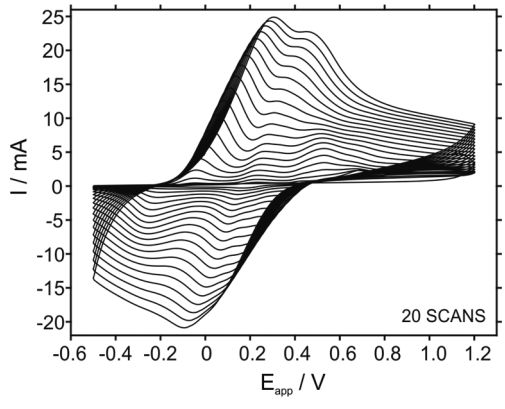

Figure 1. CVs observed during PANI electropolymerization on ITO glass substrate. Scan rate = 100 mV s^{-1}.

DOI: 10.1021/acs.analchem.9b03402
Anal. Chem. 2019, 91, 14951−14959

polymerization of PANI on ITO glass substrate during 20 CV scans (from −0.5 to 1.2 V) in aniline/H_2SO_4 solution.[5,28−31] A detailed description of the peaks' evolution is illustrated in SI Figure S3 with individual voltammograms. The first scan displayed a peak at 1.1 V that does not appear for consecutive scans as a result of the initial oxidation of aniline.[32] Therefore, the potential window selected for the PANI electropolimerization up to 1.2 V is in principle adequate. Certainly, all the observed peaks in subsequent CV scans may be attributed to different mechanisms occurring along the PANI elecropolymerization. The first (−20 mV) and last (700 mV) peaks displayed in the second scan are assigned to transitions involving LE-E and E-PN structures, respectively.[33] The other two peaks (at 230 and 430 mV) are associated with certain degradation processes in the PANI film, mainly including hydrolysis reactions.[34,35]

As the number of CV scans increases, the four anodic peaks initially observed in the second scan at −20, 230, 430, and 700 mV change as follows. The first and second peaks increased and gradually shifted to more positive potentials, while the third one increased up to the 10th scan, and the fourth one (700 mV) decreased and overlapped with the third peak. From the 10th scan, once both peaks merged, this new peak tended to decrease, and was not visible anymore from the 13th scan. Importantly, the increase of the third peak together with the decrease in the fourth one point out a degradation of the PANI film likely owing to overoxidation at high potentials. The merging of these peaks in only one results in an increased anodic−cathodic peak separation and therefore, an increase in the resistance of the electrode. Considering the final application of the developed PANI film as a proton source, most probably, PANI performance could be further improved by tuning the electropolymerization process in order to avoid the described degradation, if necessary.

The formation of the PANI film was monitored by spectrophotometry (using the cell shown in Scheme 1a). As an example, the absorbance registered during the first and second scans are shown in SI Figure S4a and b, respectively. In addition, the absorbance recorded for increasing number of scans at 420 and 700 nm is presented in SI Figure S4c. The anodic wave at 1.1 V in the very first anodic scan (SI Figure S3a) coincides with the initial increase in absorbance showing a predominant band with a maximum at 420 nm, which indicates the start of the formation of PANI related to the presence of aniline radicals and dimers.[31] During the cathodic scan, this peak at 420 nm remained almost constant, whereas there is one at 700 nm that increased up to an applied potential of 200 mV and then gradually decreased displaying a maximum in absorbance.

Essentially, the band observed at 420 nm is assigned to polaron to π^*-bond transition and that at 700 nm is related to a π to polaron transition,[35] being both indicative of the presence of partially oxidized PANI structures. Thus, these two bands are in principle ascribed to the ES form (semiquinone radical present at pH 0.7 in the H_2SO_4/KCl solution),[8,9] with the last peak appearing commonly at 750−800 nm rather than 700 nm.[5,35] This shift in the peak position likely indicates that the PANI film experiences a decrease in the conjugation length due to its partial degradation during the synthesis, as above-mentioned (overoxidation at high potentials). Over consecutive CV scans, the increase of the bands at 200 and 700 mV indicate the continuous growth of the PANI film (see SI Figure S4c).[5,35]

Study of the PANI Film by Spectroelectrochemistry and Synchrotron-Based Measurements. Figure 2a presents the spectra of the PANI film polarized at different potentials during 300 s in acidic medium (pH 0.7) while that for the nonpolarized film as prepared and after overnight conditioning is shown in SI Figure S5a. Note that the PANI film was prepared with 5 CV, in principle not presenting degradation due to overoxidation. The nonpolarized PANI film displayed a main band at 420 nm, which is associated with the presence of ES. After overnight conditioning, this band decreased likely due to a higher presence of LE structure (nonconducting PANI form) in the film. Indeed, LE is the predominant form at a polarization potential of −0.5 V, as seen in Figure 2a (spectrum with no bands).

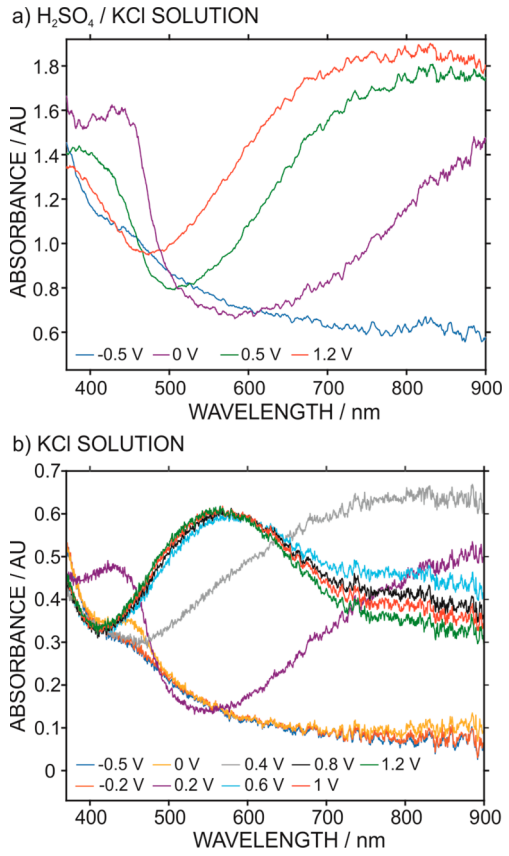

Figure 2. (a) Spectra of the PANI film in 0.5 M H_2SO_4/0.1 M KCl solution after polarization at different potentials. (b) Spectra of the PANI film in 0.1 M KCl solution after polarization at different potentials. Polarization time = 300 s.

A band at 460 nm (associated with ES) was evident with a polarization at 0 V, together with a broad band at higher wavenumbers. Then, at increasing applied potentials, both bands shifted to smaller wavenumbers, with the first band decreasing and the second one being slightly higher and narrower. This behavior is typical of the increasing presence of imine groups in the PANI film (mainly PN structures).[5,35] Accordingly, LE−E−PN redox conversion is evidently occurring through increasing polarization potentials, but the spectra trends change with the solution pH.

Figure 2b depicts the spectra displayed by the PANI film subjected to different potentials in 0.1 M KCl solution (pH 5.7). The band at 460 nm again appeared for the PANI as prepared and after overnight conditioning in KCl (SI Figure

DOI: 10.1021/acs.analchem.9b03402
Anal. Chem. 2019, 91, 14951−14959

S5b). The presence of LE structure was evident at −0.5 and −0.2 V. Then, the band at 460 nm appeared again at applied potentials of 0 and 0.2 V, while the broad band at 600−900 nm was clearly present only for 0.2 and 0.4 V. This latter band further shifted to a sole peak at 570 nm and remained constant for increasing applied potentials (up to 1.2 V). This peak was not displayed in acidic medium, and therefore pointed out a difference in the path for structural changes in the PANI at pH 5.7 than that in acidic medium. Importantly, the peak at 550 nm has been previously ascribed to the presence of quinoid structures in the PANI film (such as EB, PNB, and PNS),[36,37] and additionally, this band is known to change with dopant concentration and nature, being linked to polaron-π^* transitions in doped PANI.[38] So that, this peak can be associated with the presence of either PNS and/or PNB.

Finally, all the described trends in both media were found to be rather the same for conditioned PANI films compared to nonconditioned ones (SI Figure S5c and d). While it is clear that the PANI experiences different structural changes depending on the pH medium, more insights may arise from the subsequent interpretation of synchrotron-based measurements.

The N 1s edge NEXAFS spectra for electropolymerized PANI on glassy carbon (GC) substrate subjected to different potentials in KCl solution are presented in Figure 3a. There is a —C═N N 1s-π^* resonance at 397 eV, —NH^+ N 1s-π^* resonance at 398 eV, and —NH N 1s-σ^* resonance at 402 eV, together with a —C═N N 1s-delocalized π^* resonance at 400 eV.[39] All of the samples possess a background level of —C═N species, which may have arisen from the oxidation/degradation of the PANI samples during its preparation, handling and/or measurements. For applied potentials higher than 0 V, the —NH^+ N 1s-π^* peak intensity is relatively constant until it diminishes significantly at 1.0 V, with the —C═N N 1s-π^* peak increasing gradually. Note that the —NH^+ peak could be also ascribed to the radical N 1s, as previously demonstrated in the literature.[40] At 1.0 V, the main peak is related to the presence of the —C═N species, which is reflected by the —C═N N 1s-π^* peak passing through an intermediate oxidation state at 0 and 0.6 V. Indeed, a small peak ascribable to the —C═N N 1s-delocalized π^* or semiquinone resonance only assumed prominence at 1.0 V.

The SR-XPS N 1s spectra shown in Figure 3b and c mainly revealed —C═N binding at ca. 398 eV, —NH at ca. 400 eV along with protonated —C—NH and —C═N groups at about 401 and 402 eV, respectively.[41] By rigorously fitting these components to all of the N 1s SR-XPS spectra, we have determined the —C═N/—C—NH (imine/amine) mol ratios in all the samples (SI Figure S6). The results suggested that all the PANI forms are present at all the applied potentials, being the major ones LE and/or E structures at −0.5 and 0 V (0.3:1.0 imine/amine), E/PN structures at 0.6 V (0.8:1.0 imine/amine) and PN structures at 1.0 V (1.7 imine:1 amine). The results observed in the density of states (DOS) near to Fermi edge in the valence band spectra (VBS) confirmed that the protonated forms of PANI are less prevalent at higher applied potentials (see SI Figure S7). The rest of the analysis of the SR-XPS data is in agreement with the preparation of the PANI samples (SI Table S1).[42]

According to all the described observations up to now and considering the acid−based equilibrium of each PANI redox structure (i.e., LE, E, and PN), we may hypothesize the structural changes occurring at increasing applied potentials in the PANI film in KCl medium (pH 5.7). First of all, nonpolarized films and films polarized at mild potentials mainly contain ES (the band at 460 nm in the regular spectrum and molar ratio of imine < amine in synchrotron experiments). At high polarization potentials (from 0.6 V), there is only one band at 550 nm (associated with quinoid structures and polaron-π^* transitions in doped PANI) in the regular spectrum. Then, there is imine ≈ amine at 0.6 V, which would be in principle compatible with the presence of EB or ES/PNS mixtures, and imine > amine at higher potentials due to the higher level of PN structures.

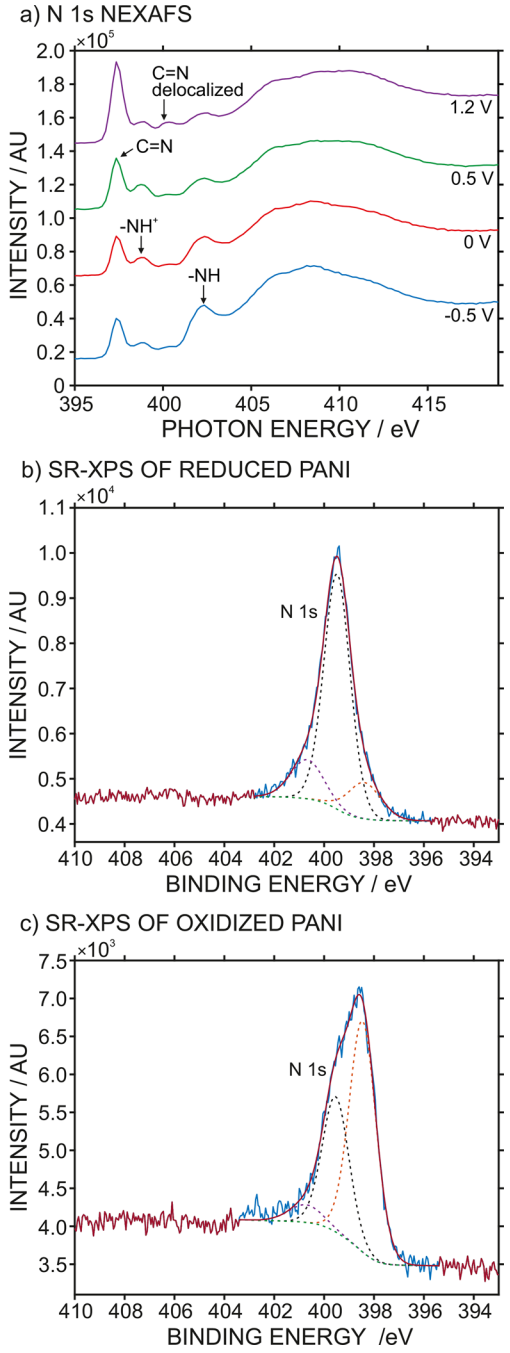

Figure 3. (a) NEXAFS N 1s spectra of PANI films polarized at different potentials. (b) SR-XPS N 1s core level spectra of the PANI film. (c) SR-XPS N 1s core level spectra of a PANI film. Polarization time = 300 s.

DOI: 10.1021/acs.analchem.9b03402
Anal. Chem. 2019, 91, 14951−14959

The presence of salt/base forms in the different PANI structures depends on the pH medium and pK_a of each individual equilibrium. Notably, these pK_a values vary dramatically according to the method used for the PANI preparation, especially for the ES−EB equilibrium, but general trends could be established here in order to try to interpret our experimental observations. Accordingly, for the base forms, LEB is expected to appear at pH ca.3, EB at pH ca. 4−7, and PNB at pH ca. 6−7.[5,8,9,35,43] Considering these values, the more stable forms at pH 5.7 would be LEB, ES/EB, and PNS. Thus, at polarization potentials from 0 to 1.0 V in KCl, ES−PNS transition is likely occurring, with the associated proton release. This agrees with the initial content in ES and the final obtention of a quinoid-base doped structure that is stable at pH 5.7.

At pH values higher than 7 in the sample solution (i.e., some environmental water samples), the presence of both EB and PNB in the PANI film is more probable and therefore, the working mechanism will expectably occur through ES−EB−PNB or even EB−PNB directly. Conversely, the most widely accepted mechanism in highly acidic medium is LEB−ES−PNB (see SI Figure S1).[5,8,9]

It is here anticipated that, according to our experiments in which we monitored the pH in thin layer samples comprising the immediate vicinity of the PANI film (see next section), PANI films polarized at either 0.2 and 0.6 V during 300 s presented rather similar final pH and therefore, the proton release occurs similarly at these two potentials. This somehow confirms the sole ES−PNS transition involving proton release at 0.2−0.6 V.

Evaluation of the pH Change in Thin Layer Samples Generated by Polarized PANI Films. We designed a flow cell to host two screen-printed PANI electrodes (i.e., one acting as a proton source and the other as a pH sensor) comprising a thin layer gap (thickness of ca. 100 μm) where the sample is renewed by a peristaltic pump (Scheme 1b), so as to explore the acidification ability in thin layer samples by using polarized PANI films.

PANI films prepared with 15 and 50 CVs were subjected to polarization at 0.6 V during 30 s in 10 mM KCl sample (initial pH of 5.7), noting that previous work on PANI films revealed an amelioration in the gradual degradation of PANI when using potentials higher than 0.75 V during time-based polarization.[43] The pH sensor was first calibrated to allow the conversion of the recorded potential into dynamic pH in the thin layer sample.

Figure 4a shows the change in the EMF of the pH sensor before, during and after the application of 0.6 V for 30 s using a PANI film made of 15 scans. First, the EMF is constant (53 mV), reflecting the initial pH of the sample (10 mM KCl, pH 5.7). Subsequently, the applied potential (0.6 V for 30 s) imposes a concentration gradient of protons from the PANI surface that extends into the entire thin layer sample by mass transport until equilibration. This process is fast according to the theory established for mass transport in samples of thickness of less than 100 μm.[44−46] When the protons reach the surface of the pH sensor, the EMF increased and then stabilized at 190 mV (pH of 3.0). Afterward, the EMF slightly decreases with time as a result of lateral diffusion of protons inside the fluidic system. Finally, the KCl sample is renewed in the thin layer sample until the EMF decreases to a value corresponding to the pH of the KCl solution.

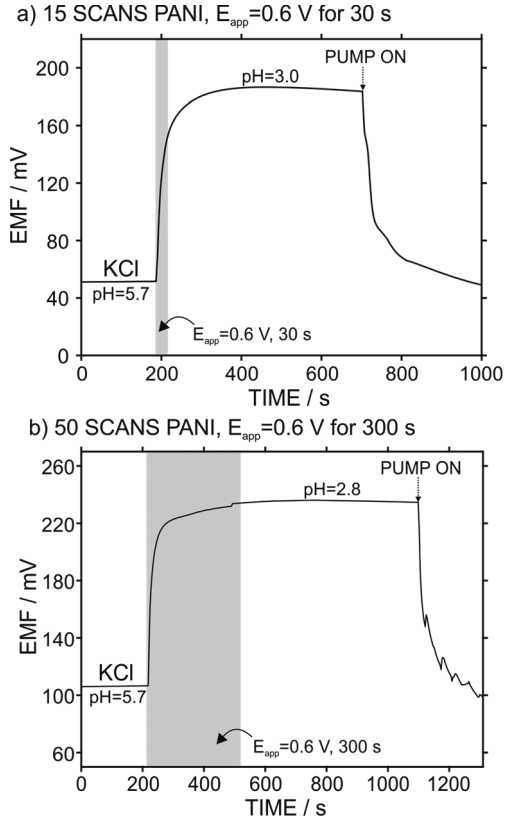

Figure 4. (a) EMF of the pH sensor in the thin layer electrolyte exposed to the PANI proton releasing film (made of 15 CVs) polarized at 0.6 V for 30 s. (b) EMF of the pH sensor in the thin layer electrolyte exposed to the PANI film (made of 50 CVs) polarized at 0.6 V for 300 s. Gray squares indicate the application of the pulse.

A similar trend was presented for the PANI film prepared with 50 CVs, with the final pH of 3.0 (Figure 4b). Importantly, during the application of the pulse, the associated current profile was registered with both PANI films (SI Figure S8 blue curve for the PANI made of 50 CVs). At the end of the polarization pulse the current was distant from zero, pointing out that the process occurring in the PANI film did not involve exhaustive depletion of the available charge.[47,48] Consequently, the time for application of the pulse was extended to 300 s with the corresponding current decay displayed at a final value of 6 μA (SI Figure S8, black line). A pH of 2.8 was reached in this case (Figure 4b).

Comparing the integrated charges from PANI films prepared using 15 and 50 CVs and polarized at 30 and 300 s, the shorter pulse comprised ca. 40−50% of the charge integrated from the longer one (for example 6.04 versus 15.11 mC for 30- and 300-s polarization of PANI made of 50 scans). This change in the released charge from the same PANI film at a longer time is linked to a change in the final pH of 0.2 units, which is not a big change in terms of acidification, manifesting that the highest pH change (i.e., proton release) mainly occurs over the initial time in which the potential is applied.

In reproducibility studies, whether consecutive pulses were applied using the same PANI film to acidify different plugs of the same sample (10 mM KCl), the final pH gradually changed never reaching the larger pH change of a freshly prepared PANI. For example, with a PANI (50 CVs) polarized at 0.6 V for 30 s, the final pH changed from 2.7 in the first pulse, to 2.8,

DOI: 10.1021/acs.analchem.9b03402
Anal. Chem. 2019, 91, 14951−14959

2.9, 3.2, and 3.7 in the second, third, fourth, and fifth pulses (see SI Figure S9a).

The incorporation of a regeneration step between pulses (application of 0 V for 60 s in 0.01 M H_2SO_4) did not allow attainment of the same pH change as in the initial pulse. In addition, the decay in current revealed a decrease in the integrated charge during consecutive pulsing. Accordingly, there were side reactions at 0.6 V that dynamically degrade the PANI film performance. Furthermore, we detected that the pH sensor was also somehow affected by the application of 0.6 V pulses, drastically changing its limit of detection and linear range of response after each pulse (from 10^{-7} M to 10^{-4} M for the limit of detection, from (6−2) to (4.2−2), SI Figure S9b and c, respectively).

It is herein suggested for the first time that thin layer samples may be easily acidified to pH values lower than those required in the determination of alkalinity (pH 4.0) by using an all-solid-state PANI film polarized at 0.6 V. While the proton release from the PANI film is an efficient process at an applied potential of 0.6 V, this is accompanied by side reactions that gradually degrade the PANI, so that the original proton release is not achieved in consecutive pulses, even though a regenerative pulse is applied. In addition, the tested conditions seem to affect the pH sensor bringing into question the pH measurements close to its changeable limit of detection.

Optimization of the Electrochemical Protocol toward a Reliable Acidification of Environmental Water Samples. To avoid the aforementioned degradation of the PANI at 0.6 V, we also completed experiments at 0.2 V, a potential that is sufficiently positive to allow proton release via the conversion of ES to EB forms while avoiding side reactions. Figure 5a presents the final pH observed in 10 mM KCl solution after acidification with a PANI film (prepared with 50 scans) polarized at 0.2 V over increasing time. It is evident that longer times are needed to reach the same acidification efficiency as with the application of 0.6 V (i.e., for a final pH close to 3, it is needed a time of 30 and 480 s using 0.6 and 0.2 V respectively). However, a time between 120 and 480 s will allow, in principle, the detection of alkalinity in samples at pH 4.0.

To check whether the efficiency for the proton release is enough to break the natural buffer in environmental water samples, thereby leading to sample acidification, we completed a series of experiments using tap water. The application of 0.2 V for 300 s in tap water led to a final pH of 3.1 ± 0.1 (SI Figure S10), as the average of four consecutive pulse experiments. Notably, the regeneration pulse (0 V for 450 s in 1 mM H_2SO_4) applied after each proton release step is now sufficient to drive the PANI film back to its initial state where the ES/EB forms are predominant. After the 0.2 V polarization, it is possible to reversely convert the PNS into ES, while it was not possible at 0.6 V because of side reactions that degrade the PANI film.

The optimized protocol for sample acidification (i.e., 0.2 V for 300 s and regeneration at 0 V for 450 s) was applied to artificial samples containing different carbonate concentrations. In principle, the released number of protons (or charge) is always the same at a fixed potential and time. Thus, for different carbonate concentrations, it is expected to have a distinct final pH according to the following approach (see SI Figure S11): the initial concentration of carbonate (or, in general terms, any base present in the thin layer sample) will

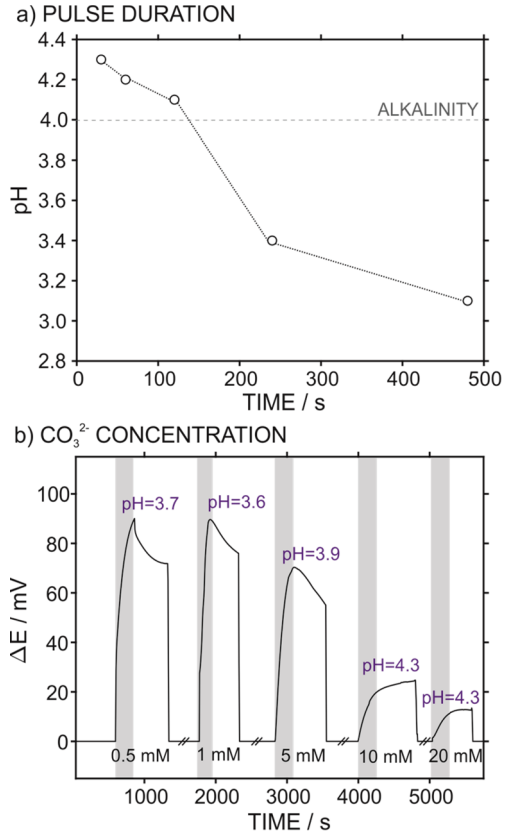

Figure 5. (a) Final pH observed in 0.1 M KCl solution after acidification using a PANI film (made of 50 CVs) polarized at 0.2 V for different time periods. (b) EMF of the pH sensor corresponding to acidification of synthetic carbonate-based samples. The discontinuity lines show the place in which the regeneration step was accomplished (E_{app} = 0 V for 450 s). The pH values in the plots are indicative of the final pH reached in each sample. Gray squares indicate the application of the pulse.

be gradually reduced with the release of protons to the sample as a result of acid−base neutralization. Once the total moles of carbonate (or any base) are consumed, the rest of released protons will provoke acidification of the sample (i.e., the amount of "free protons" will be dependent on the carbonate concentration in the solution).

As expected, at higher carbonate concentrations, the final pH is not diminished as much under the same acidification conditions (Figure 5b). In addition, with samples at carbonate concentrations in excess of 5 mM, longer pulses would be necessary to reach pH 4.0 to allow the detection of alkalinity. Conversely, 300 s is sufficient for a carbonate concentration in the range of 0.5−5 mM. In principle, this range is compatible with the majority of environmental waters according to EPA levels, noting that the alkalinity in ground and lake water ranges from 30 to 500 mg CO_3^{2-} L^{-1} (ca. 0.5−8 mM CO_3^{2-}) in river from 10 to 300 mg (ca. 0.1−5 mM) and in seawater from 120 to 150 (ca. 2.3−2.6).[49,50] However, water from contaminated sources, may present higher alkalinity values,[51] and most probably, different PANI films—with higher acidification efficiency—would be necessary. Furthermore, the longer time required for acidification of samples with higher base content (or higher alkalinity) is likely coming from the need of a larger number of protons for the acid−based local titration but also from a hindering of the electron transfer

DOI: 10.1021/acs.analchem.9b03402
Anal. Chem. 2019, 91, 14951−14959

in the PANI film. Notably, at high pH values, the most probable mechanism for the proton release is EB-PNB and therefore, the conductivity of the PANI film will be lower than in more acidic pH medium, in which the PANI film will be mainly based on the ES form.

Advantageously, the possibility of sample acidification is not restricted to alkalinity detection but is also suitable for other applications. Indeed, acidification is a required pretreatment in many analytical detections. For example, it has been recently published that sample acidification is needed to lower the hydroxyl ion content in environmental water prior to macronutrient analysis (NO_3^- and NO_2^-) using potentiometric ion-selective electrodes.[52,53] Acidification was accomplished using an in-line unit based on protonated-dialysis membranes for passive proton exchange with the sample.[52] However, this approach requires a constant flow of sample since the only way of modulating the acidification level is through sample flow. This may be an inconvenience for the subsequent detection technique. Apart from solving this problem, our approach is suitable for other kinds of samples beyond the realms of environmental waters.

Regarding the effect of specific chemicals present in real water samples in the developed concept, dopant ions (i.e., anions) will participate in the LE-E-PN transitions (as depicted in SI Figure S1).[5,43,54] However, because in our experiments we are always monitoring the pH change in the thin layer sample, even if different kinetics are associated with different anions, this would not affect alkalinity detection. For sample acidification, different compositions would need different times to reach the same final pH, as a result not only of possible changes in the PANI internal transformations (including doping processes) but also the different composition in basic species (responsible for the initial pH of the sample).

Fast Alkalinity Detection in Environmental Water Samples. The developed device was herein applied to the detection of alkalinity in real samples. Acid–base titrations based on the discrete modification of pH values following the incremental addition of acid titrant, or the injection of increment of protons, are the only two approaches that have been used in the on-site detection of alkalinity (i.e., at site close-to-shore, but not in situ). With our new electrochemical approach, it is possible to perform fast alkalinity measurements (ca. 15 min per sample) with compatibility for in situ measurements.

For this purpose, the following steps are required, just after calibration of the pH sensor: (i) polarization of the PANI film (E_{app} = 0.2 V for 300 s) in contact with the thin layer sample and continuous monitoring of the EMF by the pH sensor; (ii) conversion of the dynamic EMF into dynamic pH in the sample by means of the previous calibration graph; (iii) conversion of the current decay observed during the polarization of the PANI film into accumulative charge released from the film (i.e., chrono-coulogram); (iv) combination of the charge and pH readouts (pH-coulogram). The latter curve constitutes a fast autotitration of the sample by providing the dynamic pH values. The total amount of protons released at pH 4.0 (as deduced from the associated charge) is expressed as the carbonate concentration or the alkalinity of the sample. The integrated area under the current–time curve (in μC) until the exact moment at which pH 4.0 is measured in the thin layer sample is transformed first into the number of mols of released proton. This is indeed equal to the numbers of moles of titrated base that are finally expressed as carbonate concentration in the sample. This last part of the calculations is the same as in regular acid–base titrations

Figure 6 shows the pH-coulogram for tap water and lake water samples as well as the procedure to calculate alkalinity.

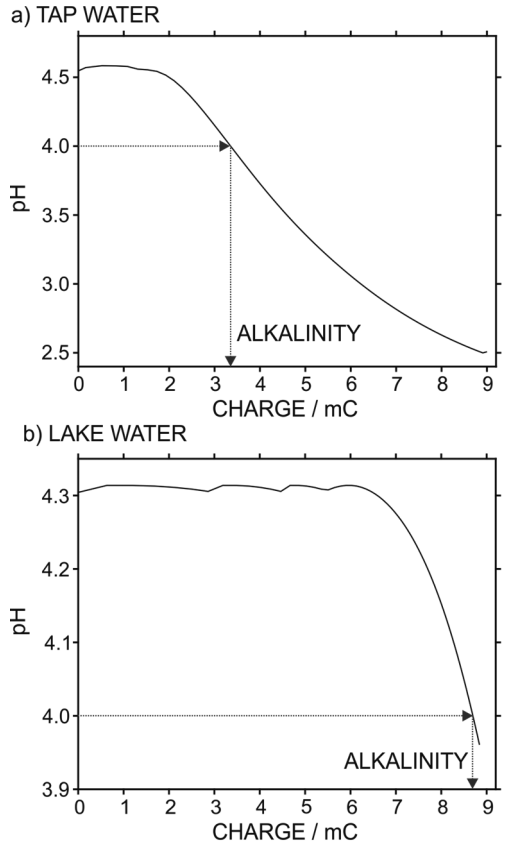

Figure 6. Plot of the pH versus released charge of protons during acidification of (a) tap water and (b) lake water. Notably, the initial pH measured with the sensor does not correspond to the initial pH of the sample because of the limit of detection of the sensor.

Each sample was analyzed in triplicate and the alkalinity was determined in parallel by using a conventional acid–base titration method. The observed alkalinity values are presented in Table 1 together with those obtained on synthetic water

Table 1. Alkalinity Detection in Water Samples[a]

	alkalinity/mM CO_3^{2-}		
sample	our method	titration	added
tap water	1.03 ± 0.13 (62.8)	1.35 ± 0.03	
lake water	2.65 ± 0.07 (160.6)	3.04 ± 0.02	
sample 1	0.49 (30.1)		0.50
sample 2	0.97 (55.2)		1.0

[a]Values expressed in mg of carbonate per liter are indicated in brackets.

samples comprising known amounts of carbonate. There was a good agreement between the alkalinity values of the autotitration and the conventional titration method in tap and lake water samples (about 10–20% relative difference).

While the conventional titration experiments were accomplished under constant stirring and the sample was in contact with air, the autotitrated sample was isolated from the

DOI: 10.1021/acs.analchem.9b03402
Anal. Chem. 2019, 91, 14951–14959

environment in the fluidic cell (i.e., the procedure of sampling + storage in a close bottle + introduction in the fluidic cell provides a different equilibration of the sample with air). This likely justify any difference found between both methods. Indeed, the alkalinity measured in the synthetic samples with known amounts of carbonate yielded close to expected values, confirming the excellent accuracy of the developed method.

Comparing the tap water and lake water sample data, while a polarization time of 300 s was sufficient to reach a pH of 4.0 in both samples, in the case of the tap water (see Figure 6a), the full titration curve yielded a final pH of 2.5. We are aware of the limitation of the use of the PANI-based pH sensor to analyze the initial pH of the samples but still, the linear range of response (from ca. pH 5 to 2.0) is more than sufficient to enable detection of pH 4.0.

The issue of limited pH sensitivity of the PANI sensor could be solved by using a handmade screen-printed electrode based on a pH selective membrane in a next generation of the fluidic cell. While this new design would be suitable for in situ measurements in a wider range of aquatic resources, the scope of this paper was to demonstrate the applicability of the fluidic cell and commercially available screen-printed electrodes in the detection of alkalinity. In the further design (second generation for the prototype), it would be convenient to explore different protocols for the PANI preparation (i.e., sequential scanning within different potential windows and also potentiostatically among others) in order to provide more conductive and controlled PANI films, toward the desired supramolecular structure and properties (including reduced need for regeneration).

Overall, besides the employment of the developed concept and fluidic device for the acidification of any water sample, the excellent results observed in this work highlight the significant potential of this method for in situ measurements of alkalinity in environmental waters. To this end, it is possible to implement a device of this nature into a submersible probe probably comprising the mentioned second-generation prototype, and test it with a large range of water samples together with a massive validation based on in situ measurements in aquatic systems. Undoubtedly, the approach presented herein constitutes a major step in the development of reliable methodology for in situ measurements of alkalinity of environmental waters.

CONCLUSIONS

Evidence of electrochemically driven proton release from PANI films are demonstrated using several characterization techniques. Spectroelectrochemical and synchrotron-based measurements provided information on the states of PANI present at different polarization conditions. Proton release from polarized PANI films was additionally quantified in water samples confined into a thin layer configuration by using a pH sensor: two faced planar PANI electrodes, one working as a proton source and the other one as regular pH electrode, were implemented in a newly designed microfluidic cell allowing not only for effective sample acidification but also for the further acid−base autotitration of the sample. The impact of this approach will be related to the implementation of a second-generation device for alkalinity detection and/or acidification in submersible probes for in situ assessment of water monitoring.

ASSOCIATED CONTENT

Supporting Information

The Supporting Information is available free of charge on the ACS Publications website at DOI: 10.1021/acs.analchem.9b03402.

Experimental section. Calibration of the pH sensor. Additional voltammograms. Additional synchrotron measurements. Illustration of the mechanism for alkalinity detection (PDF)

AUTHOR INFORMATION

Corresponding Author

*E-mail: gacp@kth.se.

ORCID

Maria Cuartero: 0000-0002-3858-8466

Roland De Marco: 0000-0002-1357-3727

Gaston A. Crespo: 0000-0002-1221-3906

Notes

The authors declare no competing financial interest.

ACKNOWLEDGMENTS

We acknowledge the financial support of KTH Royal Institute of Technology (K-2017-0371) and the Swedish Research Council (Project Grant VR-2017-4887). This project has received funding from the European Union's Horizon 2020 research and innovation programme under Marie Skłodowska-Curie grant agreement no. 792824. We thank the support of the European Community's Seventh Framework Programme (FP7/2007-2013, grant agreement no 312284) for the research at the Materials Science Beamline at the Elettra Synchrotron, the CERIC−ERIC Consortium and the Czech Ministry of Education (LM2015057). Special acknowledgement to Drs. Nataliya Tsud, Kevin C. Prince and John Bradley for the assistance with the measurements. M.C. and G.A.C. acknowledge the CERIC users' grant, and RDM thanks the International Synchrotron Access Program of the Australian Synchrotron for travel funding. We are grateful for the support from Wouter van der Wijngaart and Emre Iseri with the microfluidic cell.

REFERENCES

(1) MacDiarmid, A. G. *Angew. Chem., Int. Ed.* **2001**, *40*, 2581−2590.

(2) Dhand, C.; Dattab, M.; Malhotra, B. D. *Biosens. Bioelectron.* **2011**, *26*, 2811−2821.

(3) Fratoddi, I. V.; Camettib, C.; Russo, M. V. *Sens. Actuators, B* **2015**, *220*, 534−548.

(4) Nambiar, S.; Yeow, J. T. W. *Biosens. Bioelectron.* **2011**, *26*, 1825−1832.

(5) Visakh, P. M.; De la Pina, C.; Falletta, E. *Polyaniline Blends, Composites and Nanocomposites*; Elsevier, 2018.

(6) Gicevivius, M.; Celiesiute, R.; Kucinski, J.; Ramanaviciene, A.; Bagdziunas, G.; Ramanavicius, A. *J. Electrochem. Soc.* **2018**, *165*, H903−H907.

(7) Nguyen, H. D.; Nguyen, T. H.; Hoang, N. V.; Le, N. N.; Nguyen, T. N. N.; Doan, D. C. T.; Dang, M. C. *Adv. Nat. Sci.: Nanosci. Nanotechnol.* **2014**, *5*, 045001−045006.

(8) Ping, Z. *J. Chem. Soc., Faraday Trans.* **1996**, *92*, 3063−3097.

(9) Ping, Z.; Nauer, G. E.; Neugebauer, H.; Theiner, J.; Neckel, A. *J. Chem. Soc., Faraday Trans.* **1997**, *93*, 121−129.

(10) Lindfors, T.; Ivaska, A. *J. Electroanal. Chem.* **2002**, *531*, 43−52.

(11) MacDiarmid, A. G. *Synth. Met.* **1997**, *84*, 27−34.

(12) Huang, W. S.; Humphrey, B. D.; MacDiarmid, A. G. *J. Chem. Soc., Faraday Trans. 1* **1986**, *82*, 2385−2400.

DOI: 10.1021/acs.analchem.9b03402
Anal. Chem. 2019, 91, 14951−14959

(13) Kang, E. T.; Neoh, K. G.; Tan, K. L. *Prog. Polym. Sci.* **1998**, *23*, 211−324.
(14) Neoh, K. G.; Kang, E. T.; Tan, K. L. *J. Phys. Chem.* **1991**, *95*, 10151−10156.
(15) Takashima, W.; Nakashima, M.; Pandey, S. S.; Kaneto, K. *Electrochim. Acta* **2004**, *49*, 4239−4244.
(16) Barbero, C. A. *Phys. Chem. Chem. Phys.* **2005**, *7*, 1885−1899.
(17) Yanez-Heras, J. Y.; Planes, G. A.; Williams, F.; Barbero, C. A.; Battaglini, F. *Electroanalysis* **2010**, *22*, 2801−2808.
(18) Lizarraga, L.; Andrade, E. M.; Molina, F. V. *Electrochim. Acta* **2007**, *53*, 538−548.
(19) Blinova, N. V.; Stejskal, J.; Trchová, M.; Prokeš, J. *Polym. Int.* **2008**, *57*, 66−69.
(20) Shiiazu, K.; Murakoshi, K.; Kita, H. *J. Electroanal. Chem. Interfacial Electrochem.* **1990**, *277*, 347−353.
(21) Schmidt, V. M.; Tegtmeyer, D.; Heitbaum, J. *J. Electroanal. Chem.* **1995**, *385*, 149−155.
(22) Wen, L.; Kocherginsky, N. M. *J. Membr. Sci.* **2000**, *167*, 135−146.
(23) Nath, A.; Kanungo, M.; Contractor, A. Q. *J. Electroanal. Chem.* **2003**, *557*, 119−125.
(24) Pankratova, N.; Afshar, M. G.; Yuan, D.; Crespo, G. A.; Bakker, E. *ACS Sensors* **2016**, *1*, 48−54.
(25) Afshar, M. G.; Crespo, G. A.; Bakker, E. *Angew. Chem., Int. Ed.* **2015**, *54*, 8110−8113.
(26) Udeigwe, T. K.; Eze, P. N.; Teboh, J. M.; Stietiya, M. H. *Environ. Int.* **2011**, *37*, 258−267.
(27) Cuartero, M.; Pankratova, N.; Cherubini, T.; Crespo, G. A.; Massa, F.; Confalonieri, F.; Bakker, E. *Environ. Sci. Technol. Lett.* **2017**, *4*, 410−415.
(28) Boeva, Z. H.; Sergeyev, V. G. *Polym. Sci., Ser. C* **2014**, *56*, 144−153.
(29) Sezai, S.; Ates, M.; Kilic, B. *Int. J. Electrochem. Sci.* **2008**, *3*, 777−786.
(30) Rohom, A. B.; Londhe, U. P.; Mahapatra, S. K.; Kulkarni, S. K.; Chaure, N. B. *High Perform. Polym.* **2014**, *26*, 641−646.
(31) Fomo, G.; Waryo, T. T.; Baker, P.; Iwuoha, E. I. *Int. J. Electrochem. Sci.* **2016**, *11*, 10347−10361.
(32) Wang, B.; Tang, J.; Wang, F. *Synth. Met.* **1986**, *13*, 329−334.
(33) Duic, L. Z.; Mandic, M.; Kovac, S. *Electrochim. Acta* **1995**, *40*, 1681−1688.
(34) Chen, W. C.; Wen, T. C.; Gopalan, A. *Electrochim. Acta* **2002**, *47*, 4195−4206.
(35) Xia, Y.; Wiesinger, J. M.; MacDiarmid, A. G.; Epstein, A. *Chem. Mater.* **1995**, *7*, 443−445.
(36) Jelle, B. P.; Hagen, G.; Hesjevik, S. M.; Ødegård, R. *Electrochim. Acta* **1993**, *38*, 1643−1647.
(37) Malinowski, P.; Michalska, A.; Maksymiuk, K. *J. Solid State Electrochem.* **2010**, *14*, 2027−2037.
(38) Rao, C. R. K.; Muthukannan, R.; Vijayan, M. *Bull. Mater. Sci.* **2012**, *35*, 405−414.
(39) Bulusheva, L. G.; Fedorovskaya, E. O.; Okotrub, A. V.; Maximovskiy, E. A.; Vyalikh, D. V.; Chen, X.; Song, H. *Phys. Status Solidi B* **2011**, *248*, 2484−2487.
(40) Do Nascimento, G.; Constantino, V. R. L.; Landers, R.; Temperini, M. L. A. *Macromolecules* **2004**, *37*, 9373−9385.
(41) Ullah, R.; Bowmaker, G. A.; Laslau, C.; Waterhouse, G. I. N.; Zujovic, Z. D.; Ali, K.; Shah, A. A.; Travas-Sejdic, J. *Synth. Met.* **2012**, *198*, 203−211.
(42) Moulder, J. F.; Stickle, W. F.; Sobol, P. E.; Bombden, K. D. *Handbook of X-ray Photoelectron Spectroscopy*; Perkin-Elmer Corporation Physical Electronics Division, 1992.
(43) Castrellon-Uribe, J.; Nicho, M. E.; Reyes-Merino, G. *Sens. Actuators, B* **2009**, *141*, 40−44.
(44) Zhang, H.; Li, H.; Wang, J. *Adv. Mater. Res.* **2012**, *535*−*537*, 1205−1209.
(45) Cuartero, M.; Crespo, G. A.; Bakker, E. *Chimia* **2015**, *16*, 203−206.
(46) Cuartero, M.; Crespo, G. A.; Afshar, M. G.; Bakker, E. *Anal. Chem.* **2014**, *86*, 11387−11395.
(47) Crespo, G. A.; Bakker, E. *RSC Adv.* **2013**, *3*, 25461−25474.
(48) Otero, T. F.; Grande, H.; Rodriguez, J. *Electrochim. Acta* **1996**, *41*, 1863−1869.
(49) Stumm, W.; Morgan, J. J. *Aquatic Chemistry: Chemical Equilibria and Rates in Natural Waters*; Wiley, 2012.
(50) Boyd, C. E.; Tucker, C. S. *Pond Aquaculture Water Quality Management*; Springer: Boston, MA, 1998.
(51) Duarte, C. M.; Hendricks, I. E.; Moore, T. S.; Olsen, Y. S.; Steckbauer, A.; Ramajo, L.; Carstensen, J.; Trotter, J. A.; McCulloch, M. *Estuaries Coasts* **2013**, *36*, 221−236.
(52) Pankratova, N.; Cuartero, M.; Cherubini, T.; Crespo, G. A.; Bakker, E. *Anal. Chem.* **2017**, *89*, 571−575.
(53) Cuartero, M.; Crespo, G.; Cherubini, T.; Pankratova, N.; Confalonieri, F.; Massa, F.; Tercier-Waeber, M. L.; Abdou, M.; Schafer, J.; Bakker, E. *Anal. Chem.* **2018**, *90*, 4702−4710.
(54) Alesary, H. F.; Ismail, H. K.; Khudhair, A. F.; Mohammed, Q. M. *Orient. J. Chem.* **2018**, *34*, 2525−2533.

DOI: 10.1021/acs.analchem.9b03402
Anal. Chem. 2019, 91, 14951−14959